



Published in final edited form as:

Thorax. 2022 January ; 77(1): 47–57. doi:10.1136/thoraxjnl-2020-216469.

sphingosine kinase 1 regulates lysyl oxidase through STAT3 in hyperoxia-mediated neonatal lung injury

Alison W Ha¹, Tao Bai², David L Ebenezer², Tanvi Sethi², Tara Sudhadevi³, Lizar Ace Mangio², Steven Garzon⁴, Gloria S Pryhuber⁵, Viswanathan Natarajan², Anantha Harijith³

¹Department of Biochemistry and Molecular Genetics, University of Illinois at Chicago, Chicago, Illinois, USA

²Department of Pharmacology, University of Illinois at Chicago, Chicago, Illinois, USA

³Department of Pediatrics, Case Western Reserve University School of Medicine, Cleveland, Ohio, USA

⁴Department of Pathology, University of Illinois at Chicago, Chicago, Illinois, USA

⁵Department of Pediatrics, University of Rochester, Rochester, New York, USA

Abstract

Introduction—Neonatal lung injury as a consequence of hyperoxia (HO) therapy and ventilator care contribute to the development of bronchopulmonary dysplasia (BPD). Increased expression and activity of lysyl oxidase (LOX), a key enzyme that cross-links collagen, was associated with increased sphingosine kinase 1 (SPHK1) in human BPD. We, therefore, examined closely the link between LOX and SPHK1 in BPD.

Method—The enzyme expression of SPHK1 and LOX were assessed in lung tissues of human BPD using immunohistochemistry and quantified (Halo). In vivo studies were based on *Sphk1*^{-/-} and matched wild type (WT) neonatal mice exposed to HO while treated with PF543, an inhibitor of SPHK1. In vitro mechanistic studies used human lung microvascular endothelial cells (HLMVECs).

Results—Both SPHK1 and LOX expressions were increased in lungs of patients with BPD. Tracheal aspirates from patients with BPD had increased LOX, correlating with sphingosine-1-phosphate (S1P) levels. HO-induced increase of LOX in lungs were attenuated in both *Sphk1*^{-/-} and PF543-treated WT mice, accompanied by reduced collagen staining (sirius red). PF543 reduced LOX activity in both bronchoalveolar lavage fluid and supernatant of HLMVECs

Correspondence to Dr Anantha Harijith, Pediatrics, Case Western Reserve University, School of Medicine, Cleveland, OH 44106-4915, USA; axh775@case.edu.
AWH and TB contributed equally.

Contributors AWH and TB participated in the study design, performed experiments, interpreted results, prepared figures and edited the manuscript. DLE contributed to conceptualising the study, performed experiments, interpreted results and prepared figures. TSe performed experiments, interpreted results, prepared figures and analysed data. TSu performed experiments, interpreted results, prepared figures and analysed the data and edited the manuscript. LAM performed experiments, interpreted results, prepared figures and analysed the data. SG assisted the design of the study, interpreted results and edited the manuscript. GSP guided the conceptualisation and design of the study, interpreted results and edited the manuscript. VN conceptualised the study and its design, interpreted results and edited the manuscript. AH conceptualised the study and its design, performed experiments, analysed data, interpreted results, drafted and edited the manuscript. All the authors read and approved the final manuscript.

following HO. In silico analysis revealed STAT3 as a potential transcriptional regulator of LOX. In HLMVECs, following HO, ChIP assay confirmed increased STAT3 binding to LOX promoter. SPHK1 inhibition reduced phosphorylation of STAT3. Antibody to S1P and siRNA against SPNS2, S1P receptor 1 (S1P₁) and STAT3 reduced LOX expression.

Conclusion—HO-induced SPHK1/S1P signalling axis plays a critical role in transcriptional regulation of LOX expression via SPNS2, S1P₁ and STAT3 in lung endothelium.

INTRODUCTION

Oxygen supplementation is commonly used to treat premature newborn infants with immature lungs,^{1 2} as well as critically ill older patients with respiratory failure due to conditions such as acute respiratory distress syndrome and pneumonia, including that caused by COVID-19.³⁻⁵ Though oxygen is essential to sustain life, exposure to hyperoxia (HO) causes increased production of reactive oxygen species (ROS), leading to untoward cellular injury, inflammation and, ultimately, cell death.^{6 7} Excessive ROS generation contributes to oxidant-induced lung injury in neonatal bronchopulmonary dysplasia (BPD) and the corresponding animal models.^{8 9} Preterm infants with BPD who were exposed to higher levels of supplemental oxygen in neonatal intensive care unit, so as to achieve higher oxygen saturation such as used in the STOP-ROP trial, were found to have more severe lung disease(s) on follow-up.¹⁰⁻¹² One of the most prominent mechanisms of ROS production in the pathogenesis of lung injury, including BPD, is through NADPH oxidase (NOX) activation comprising of NOX1-5 and DUOX 1–2 family members.^{9 13} We have earlier shown that reducing sphingosine-1-phosphate (S1P) production by sphingosine kinase (SPHK) 1, but not SPHK2, protected against HO-induced lung injury in both neonatal and juvenile mice.¹⁴ This differential role of SPHK1 and SPHK2 in part may be attributed to difference in the localisation, wherein SPHK1 is known to be primarily located in the cytoplasm and SPHK2 both in the cytoplasm and the nucleus of the cell.^{13 15}

Infants developing BPD have low lung compliance^{16 17} due to increased rigidity of lung parenchyma, and in animal models too, rigid lung parenchyma could contribute to increased respiratory system resistance, as reported by us earlier.¹⁸ Increased collagen cross-linking by lysyl oxidase (LOX), a matrix modifying enzyme, could also contribute to lung pathology leading to BPD, as reported earlier.¹⁹ LOX is an important enzyme that plays an active role in matrix stabilisation, essential for normal alveolar formation.^{20 21} LOX catalyses the oxidative deamination of lysine and hydroxylysine residues, generating reactive semialdehydes.^{22 23} These semialdehydes condense to form covalent cross-links in elastin and collagen molecules, providing structural stability to extracellular matrix. Increased LOX expression and/or activity is associated with BPD¹⁹ as it overstabilises the matrix, contributing to poor alveolar formation.²⁴ LOX is also associated with pulmonary fibrosis²⁵ and is emerging as a key player in eosinophilic oesophagitis.²⁶ Earlier studies have shown an increase in S1P level in tracheal aspirates (TAs) of patients with BPD.^{18 27} The significance of sphingolipids such as ceramide and S1P in the pathogenesis of BPD is being understood more recently.^{28 29} However, the causal link between SPHK1/S1P and LOX in increased interstitial collagen cross-linking, a pathological consequence in BPD, is unknown.

We observed that LOX expression is downregulated in mouse lung tissues when *Sphk1* is knocked out genetically or inhibited pharmacologically. On the contrary, genetic deletion of *Sphk2* increased hyperoxic lung injury accompanied by elevated expression of LOX in the lung tissue. In the present study, our results, for the first time, show that LOX activation in HO is mediated by increased S1P generated via SPHK1 with subsequent release of S1P through S1P transporter SPNS2, binding of S1P to S1P receptor 1 (S1P₁), activation of STAT3 to phospho-STAT3, its translocation to the nucleus and transcriptional regulation of LOX. These findings show a causal link of SPHK1/S1P/S1P₁ signalling axis in regulation of LOX through STAT3 transcriptional factor in lung endothelium.

METHODS

Human BPD tissue use (deidentified)

Neonatal human lung tissue was retrieved from archived autopsy material at the University of Rochester Medical Center (URMC) and University of Illinois at Chicago (UIC). We would like to thank the BRINDL repository at URMC for providing us the neonatal autopsy samples under IRB# STUDY00004818 and Material Transfer Agreement (MTA #4668). Deidentified human material was used with the approval of the Institutional Review Board of the UIC (Protocol #2012–1018) and based on human research protection principles espoused in the Declaration of Helsinki. The clinical characteristics of the patients from whom the specimens were derived are presented in online supplemental table 1 (patients with BPD, called the ‘BPD group’). Tissue samples were collected at autopsy, within 24 hours of death. Those who had pulmonary haemorrhage, pulmonary hypertension and sepsis/pneumonia were excluded. Both Rochester and Chicago samples were pooled for analyses. The average time between death and tissue processing was similar in all the patient groups.

Tracheal aspirates

TAs were collected from formerly premature infants who were mechanically ventilated with an in-dwelling endotracheal tube. The procedures were approved by the Institutional Review Board of the University of Illinois at Chicago (Protocol #2010–1111, ‘Consortium for Neonatal Intensive Care Unit’). Parental consent was obtained prior to collection. TAs were collected cross-sectionally from controls born at term and those meeting criteria of severe BPD when endotracheal tube lavage was performed as part of routine care. TAs were isolated from patients diagnosed with BPD and remaining intubated at 36 weeks’ postmenstrual age. Infants with BPD remained intubated and ventilated for BPD at the time of collection of TA. Samples from a total of six patients were used for the western blotting. Term healthy infants (controls) were intubated for elective procedures such as repair of myelomeningocele, inguinal hernia or anorectal malformation. They had no pulmonary conditions. Aspirate specimen were centrifuged and supernatants stored at –80°C. BPD and its severity were defined as per National Institutes of Health consensus criteria.^{30 31} Select clinical details are shown in online supplemental table 2. LOX is an enzyme secreted into the extracellular matrix, and hence, we performed western blotting of the TAs to determine relative expression levels. Normalised samples for protein content were used for immunoblotting. The protein concentration range was 0.42–0.65 mg/dL in normal and 0.36–

0.95 mg/dL in preterm infants with BPD. TAs stained with blood were eliminated from analyses.

Immunohistochemistry

Deidentified paraffin-embedded human lung tissues were studied by immunohistochemical staining for the expression of LOX using rabbit anti-LOX antibody (Thermo Fisher PA-116955) at 1:2000 dilution and SPHK1 by staining with rabbit anti-SPHK1 (Ab 71700, Abcam, Cambridge, Massachusetts, USA) at 1:100 dilution. Specificity of anti-SPHK1 for immunohistochemistry was proven by using blocking peptide for SPHK1 (Ab 16634, 1:1000 dilution). No blocking antibody is available for LOX. LOX antibody was verified and certified by the supplier, Thermo Fisher (Waltham, Massachusetts, USA). We analysed the lung tissue excluding airways and blood vessels. Edges of lung tissue were always excluded as they tended to stain darker. Area was measured in pixels, and intensity of staining was noted. Strongly stained areas of the lung were defined as a percentage of the whole lung area so that comparison could be made between various groups.

Image preparation—Slides were scanned using Aperio AT2 (Leica Biosystems). The digital images were then imported into a project folder within Aperio eSlide Manager (Leica Biosystems). Images were annotated for analysis, with positive penning indicating regions of interest to be included from analysis and negative penning indicating regions to be excluded from analysis. Whole tissue areas were positively penned, while artefacts (folds, debris, secretions and so on) and prominent vessels and bronchi were negatively penned using Imagescope program (Leica Biosystems).³²

Positive pixel count—The image analysis tool ‘positive pixel count’ within eSlide Manager (Leica Biosystems) was used to quantify the area and intensity of positive and negative staining. The number of pixels in an image was counted and classified as either negative, weakly positive, moderately positive or strongly positive. The Positive Pixel Count has input parameters to define each colour as positive (brown) and negative (blue), in addition to defining the threshold range as weak, moderate or strong positive. Parameters were set and run batchwise, and review of analysed markup was conducted to make changes to parameter to obtain a more accurate markup. After review, batch export of data and statistical analysis was conducted.

BPD mouse models

Exposure of neonatal mice to HO results in BPD-like lung morphology characterised by alveolar simplification.^{33 34} The pups were exposed to 95% HO for 1 week, as explained in the section further.

Mouse experiments and animal care—All experiments using animals were approved by the Institutional Animal Care and Use Committee at University of Illinois at Chicago (protocol #15–246). We used neonatal mouse pups to study the effect of HO in the developing lungs.¹⁴ *Sphk1*^{-/-} and *Sphk2*^{-/-} mice, were obtained from Dr Richard L Proia (NIDDK, National Institutes of Health, Bethesda). These mice were backcrossed to C57BL/6 background for two generations (F2 hybrid). The resultant mixed background of

C57BL/6 strain and the original background (F2 hybrid) was used as controls and is referred to hereafter as wild type (WT). WT, *Sphk1*^{-/-} or *Sphk2*^{-/-} newborn (NB) mice along with the lactating dams were exposed to HO or normoxia (NO) from postnatal (PN) day 1 for 7 days as previously described.¹⁸ The lactating dams were rotated between HO and NO every 24 hours. PF543 is a specific inhibitor of SPHK1.³⁵ We administered PF543 at a dose of 5.0 mg/kg on alternate days as published earlier.¹⁸ The mice pups requiring injection with PF543 had to be injected intraperitoneally a volume of 20 μ L, which was better tolerated on PN 3 compared with PN 1. Mice pups were pretreated with PF543 or vehicle and exposed to NO or HO (95%) from PN days 3–10 (online supplemental figure 1). A total of four doses was given between PN 3 and 10. At the end of experiments, the animals were sacrificed, and lung tissues were collected and prepared for further analysis.

Bronchoalveolar lavage (BAL) collection—BAL collection with PBS was performed, as previously described.¹⁴ Protein concentration in BAL fluids collected were measured using Bio-Rad Protein Assay (Bio-Rad, Hercules, California, USA).¹³

Preparation of S1P for exogenous addition on endothelial cells—S1P dissolved in methanol:toluene (1:1 v/v) to a final concentration of 1 mM was stored in aliquots in glass vials at -20°C . An aliquot of S1P solution was transferred to a glass tube; the solvent was evaporated under N_2 to leave a thin film of S1P at the bottom of the glass tube, which was reconstituted by sonication with probe sonicator (3×15 s) in basal EGM-2 medium containing 0.1% fatty acid free bovine serum albumin. The S1P solution was made fresh 10 min prior to the experiment and kept at room temperature.³⁶

Histological analysis—Animals were euthanised, and lungs were collected to be processed for histological evaluation as described earlier.³⁶ The tissue was stained with H&E or sirius red and methyl green at ‘Research Histology Laboratory’ (Department of Pathology at University of Illinois, Chicago). Sirius red specifically stains cross-linked collagen types I and III fibrils, directly indicating the deposition of mature collagen in lung tissue, an indication of the function of LOX.^{37,38} The objective assessment of alveolarisation was determined by the mean linear intercept (MLI) method.¹⁸ Slides were examined at $10\times$ magnification and the MLI for a minimum of 50 alveoli for each section were measured. At least three sections from each pup were used for analysis. Higher magnification ($40\times$) was used to examine collagen deposition in lung tissue.

Endothelial cell culture—Human lung microvascular endothelial cells (HLMVECs) (Lonza, Morristown, New Jersey, USA), with passages between 5 and 8, were cultured in EGM-2 complete media (10% foetal bovine serum (FBS), 100 units/mL penicillin and streptomycin) at 37°C and 5% CO_2 . They were grown to about 90% confluence when cultured in 35 or 60 mm dishes or on glass cover slips for various studies as described earlier.¹³

Exposure of cells to HO—HLMVECs ($\sim 90\%$ confluence) in complete EGM-2 medium were placed in the cell culture incubator at 37°C for HO (95%) exposure as described earlier.¹³ The concentration of O_2 inside the Billups-Rothenberg modular incubator chamber was monitored using digital oxygen monitor. The buffering capacity of the cell culture

medium did not change significantly during the period of HO exposure and was maintained at a pH ~7.4.

Immunoblotting—Protein expression was detected in the mouse lungs and HLMVECs by immunoblotting, as described earlier.^{13 14} HLMVECs grown on 35 mm dishes (~90% confluence) were used in experiments for HO, lysed and subjected to immunoblotting as described earlier.^{13 14} The following antibodies were used: LOX (PA1-16955, Fisher Scientific), SPHK1 (Ab37980, Abcam), P-STAT3 (9145S, Cell Signaling), STAT3 (4904P Cell Signaling), SPNS2 (NBPI-54345, Novus Biologics), GAPDH (sc-25778, Santa Cruz Biotechnology), Actin (A15441, Sigma Aldrich) and EDG1 (S1P₁) (sc-25489, Santa Cruz Biotechnology). The following siRNAs from Santa Cruz Biotechnology were used: *STAT3* siRNA (sc-29493), *SPNS2* siRNA (sc-106749), *SIP₁* siRNA (sc-37086), Control siRNA (sc-37007) and *SPHK1* siRNA (sc-36494). RTPCR of LOX expression (mouse) used primers: 5'-ATGCGTTTCGCCTGGGCTGTGC-3' (forward primer) and 5'-CTAATACGGTGAAATTGTGCAGCC-3' (reverse primer).

Transient transfection of HLMVECs—In siRNA experiments, HLMVECs grown to ~50% confluence in 6-well plates were transfected with Gene Silencer transfection reagent (Gelantis, San Diego, California, USA) plus scRNA (scrambled) or siRNA specific for *SPHK1*, *SPNS2*, *SIP₁* or *STAT3* in serum-free EBM-2 medium according to manufacturer's recommendations. After 3 hours of transfection, the serum-free media was replaced by 1 mL of fresh complete EGM-2 medium containing 10% FBS and the growth factors. The cells were cultured for an additional 72 hours prior to experiments.

Pretreatment of cells with SPHK1 inhibitor, PF543—HLMVECs grown to ~90% confluence were preincubated with PF543 (1 μ M) in serum-free or media containing 1% FBS as indicated for 1 hour prior to stimulation with HO (95% O₂, 5% CO₂) for 6 hours.

LOX activity assay—Kit (Fluorometric) (Ab112139, Abcam) was used to measure LOX activity in BAL and cell culture supernatant solutions. The assay uses a proprietary red fluorescence substrate for horseradish peroxidase (HRP)-coupled reactions that estimates release of hydrogen peroxide from a proprietary LOX substrate by the action of LOX present in the sample. The relative fluorescence was determined at Ex/Em=540/590 nm in a fluorescence microplate reader as recommended. The assay is semiquantitative as there is no LOX standard for calibration. The assay is extremely sensitive to changes in activity, and according to the manufacturer, its unique detection method eliminates the interference that occurs in certain biological samples. We used LOX like 2 (LOXL-2) as standards (positive control) to ensure that the assay worked as shown in previous publications.³⁹ This was used as positive and negative control, but no attempt was made to quantify using LOXL-2 standard. LOX assay results were expressed as fold change compared with room air controls. During the activity assay, it was noted that the fluorometric method of measurement saturated at 24 min, and hence, 18 min was taken as the cut-off when the difference between various groups was most evident. Measurements were taken every 6 min.

In silico analyses of transcription factor binding sites for LOX—In silico analyses was performed using the Genomatix (Munich, Germany) software tool namely

MatInspector.⁴⁰ This tool uses a large library of matrix descriptions for transcription factor binding sites to locate matches in DNA sequences. We performed initial search for the promoter(s) of *LOX* gene in humans (*LOX* Gene ID: 4015, Homo sapiens chromosome 5). Core similarity for the search was set at the default of 0.75. Genomatix system suggested transcripts for *LOX* were analysed for possible STAT transcription factor binding sites to the promoter. Data obtained from the in silico analyses were confirmed by ChIP assay to confirm the transcription factor binding to the promoter sequence.

ChIP assay—HLMVECs grown to 95% confluency on 100 mm dishes were serum starved in 0.1% serum for 1 hour. Dishes were exposed to 95% HO for 3 hours. ChIP assay was performed as described previously.¹⁵ We used the *LOX* promoter-specific ChIP-validated primer from Qiagen (Valencia, California, USA): EpiTect ChIP qPCR Primer Assay for Human *LOX* [GPH1024332(+)-01A] Unigene #Hs. 102267, GenBank [NM_002317](#). EpiTect ChIP qPCR Assays provide validated genome-wide real-time PCR primers specifically designed for the analysis of the specific ChIP-enriched genomic DNA.^{41 42} The validated primers focus on specific 1 kb genomic regions in gene promoters. This enables a detailed analysis of the dynamic interaction between DNA and nuclear proteins. Data obtained were analysed as fold enrichment = 2^{-Ct} .

Statistical analysis

Mann-Whitney U test was used for analysis of human IHC data. Student's t-test and two-way analysis of variance were used to compare means of two or more different treatment groups, respectively. Pearson correlation was used to measure the linear correlation between *LOX* content of TA and S1P level. The level of significance was set to $p < 0.05$ unless otherwise stated. Results were expressed as mean \pm SEM.

RESULTS

SPHK1 and *LOX* expressions are upregulated in neonatal BPD lung tissues

Both SPHK1 and *LOX* have been independently implicated in BPD pathology^{14 18 19 24}, however, a potential relationship between the two is unknown. As a first step to evaluate this link, we examined the expression of SPHK1 and *LOX* in formalin-fixed paraffin-embedded lung tissue sample from five control and eight BPD subjects by immunohistochemistry. Controls selected were of comparable postmenstrual age with no BPD. Patients with BPD had a significant increase in SPHK1 as evidenced by an increased area (percentage) of tissue positive for SPHK1 staining in BPD (17.5 ± 1.3) compared with controls (10.5 ± 0.8) (figure 1A,B). Area of lung tissue positive for *LOX* was also significantly elevated in BPD (26.3 ± 3.3) compared with controls (10.0 ± 2.1) (figure 1C,D). We have earlier shown that S1P was elevated in TAs of patients with severe BPD, which correlates with enhanced SPHK1 expression in lung tissue.¹⁸

Increased *LOX* expression in TAs of patients with severe BPD

LOX protein was assessed in TAs obtained from intubated neonates with normal lungs as well as age-matched controls with severe BPD. Compared with controls, TAs of neonates with BPD showed increased content of *LOX* (13.2 ± 4.2 fold) (figure 1E & F). Collectively,

these data demonstrate increased LOX and SPHK1 in human BPD lung specimens and TAs. Patients with enhanced expression of LOX had elevated S1P. This increase in S1P concentration in TAs of the patients with severe BPD compared with controls was reported earlier.¹⁸ Analysis showed that increased content of LOX correlated well ($r=0.813$) with increased concentration of S1P in TA (figure 1G).

Genetic deletion of *Sphk1* attenuates HO-induced BPD-like morphology, collagen deposition and LOX expression in neonatal mouse lung

We had earlier shown that genetic deletion of *Sphk1* attenuated HO-mediated neonatal BPD in mice.¹⁴ To investigate the role of SPHK1 in LOX expression, neonatal WT and *Sphk1*^{-/-} mice were exposed to HO, and lung tissues were investigated for collagen cross linking and LOX expression. As shown in figure 2A,B, compared with WT mice, deletion *Sphk1* reduced HO-induced alveolar simplification, as well as collagen deposition as determined by area (percentage) of sirius red staining in lungs (WT HO 30.6±5 compared with *Sphk1*^{-/-} HO 7.4±1.5). Deletion of *Sphk1* showed protection against HO-induced lung injury as evidenced by improved MLI (WT RA 32.6 µm, SEM ±0.81, WT HO 66.4 µm, SEM ±1.44, *Sphk1*^{-/-} RA 33.8 µm, SEM ±0.8, *Sphk1*^{-/-} HO 55.8 µm, SEM ±0.66) (figure 2C). HO has been shown to enhance LOX expression in mouse lung¹⁹; however, the role of SPHK1 in regulating LOX expression is unclear. Therefore, we investigated the effect of *Sphk1* deletion on LOX expression. Exposure of neonatal WT but not *Sphk1*^{-/-} mice to HO increased LOX mRNA (4.30±0.08 fold) (figure 2D) and protein expression (3.2±0.4 fold increase in WT HO compared with 0.26±0.02 in *Sphk1*^{-/-} HO. WT RA is 1±0.05 fold) (figure 2 E,F) in lung tissues. Interestingly, *Sphk1* deletion had a tendency to have lower expression of LOX in mouse lungs under NO, suggesting that the expression of LOX protein is dependent at least in part on SPHK1 even in NO (figure 2E). On the contrary, lung tissue of *Sphk2*^{-/-} neonatal mice showed a significant increase in expression of LOX when exposed to HO similar to the response seen in the WT mice (12.5±0.8 fold increase in WT HO compared with 12.1±0.6 in *Sphk2*^{-/-} HO; WT RA is 1±0.03 fold) (figure 2G,H). We have earlier shown that *Sphk2*^{-/-} neonatal mice were not protected from HO-induced lung injury as compared with *Sphk1*^{-/-}. Collectively, these results demonstrate a role for SPHK1 in HO-mediated BPD and LOX expression in neonatal mouse lungs.

SPHK1 inhibitor, PF543, protects HO-induced neonatal BPD accompanied by reduced expression of LOX

Having shown a role for SPHK1 protein in LOX upregulation by HO, next, we interrogated if SPHK1 activity is essential for LOX expression. To test this, we used PF543, a specific inhibitor of SPHK1 that has been effective in ameliorating several pathologies in experimental models including BPD,¹⁸ pulmonary hypertension,⁴³ pulmonary fibrosis,^{18 44} sickle cell anaemia⁴⁵ and cancer.⁴⁶ Neonatal mice exposed to HO (95%) and treated with PF543 from PN 3–10 were protected from neonatal lung injury compared with the HO exposed group that were not treated with PF543 (figure 3A,B). This was evidenced by improved MLI (WT RA 33.4 µm, SEM ±0.68, WT HO 68 µm, SEM ±1.38, WT RA+PF543 32.6 µm, SEM ±0.81, WT HO+PF543 57 µm, SEM ±0.45). Furthermore, PF543 administration reduced HO-induced LOX expression and area (percentage) of lung tissue stained with sirius red (28.2±5 in WT HO compared with 9.6±1.1 in WT HO treated with

PF543) (figure 3C). PF543 therapy reduced LOX expression in lung tissue (5.2 ± 0.3 fold in WT HO compared with 2.3 ± 0.2 in WT HO treated with PF543; WT RA is 1 ± 0.07 fold) (figure 3D,E). LOX activity also showed a significant reduction in broncho alveolar lavage fluid (BALF) following PF543 administration (4.4 ± 0.1 fold in WT HO compared with 1.8 ± 0.2 in PF543 treated WT HO; WT RA is 1 ± 0.07 fold) (figure 3F).

Furthermore, to determine the specificity of SPHK1 inhibition, neonatal *Sphk2*^{-/-} mice were exposed to HO. Knockdown of *Sphk2* in mice had no effect on HO-induced lung injury; however, PF543 treatment showed a significant protection against HO-induced BPD in both WT and *Sphk2*^{-/-} neonatal mice (online supplemental figure 2A). This was accompanied by improved alveolarisation as evidenced by reduced MLI. *Sphk2*^{-/-} exposed to HO had enlarged alveoli (MLI of $75 \mu\text{m}$, SEM ± 1.8) compared with *Sphk2*^{-/-} exposed to HO but treated with PF543 (MLI of $59.2 \mu\text{m}$, SEM ± 1.7) (online supplemental figure 2B). These results show that blocking SPHK1 activity with PF543 reduced HO-induced LOX expression and collagen staining in lung tissue while improving alveolarisation in neonatal mice.

SPHK1/S1P/SPNS2/S1P₁ signalling axis regulates HO-mediated LOX expression in HLMVECs

HO stimulates SPHK1 and generates S1P in lung endothelial cells.¹⁴ S1P thus, generates signals either intracellularly or is transported outside the cell by an S1P transporter SPNS2 and signals by binding to G-protein coupled receptors in the lung endothelium.^{14 15} In order to investigate the role of SPHK1/S1P/SPNS2/S1P₁ signalling in LOX expression, a series of experiments were performed using HLMVECs. The role of SPHK1 in HO-mediated LOX expression in lung endothelial cells was investigated using siRNA and PF543. Addition of exogenous S1P to HLMVECs in the absence of HO enhanced expression of LOX at 6 hours (5.7 ± 0.3 fold) with no further increase noted by 24 hours (figure 4A,B). Similarly, exposure of HLMVECs to HO enhanced LOX expression (2.4 ± 0.1 fold) that was attenuated by downregulation of SPHK1 with *SPHK1* siRNA (0.8 ± 0) or inhibiting SPHK1 activity with PF543 (5.9 ± 0.1 fold following HO reduced to 0.8 ± 0.02 fold by PF543) (figure). In addition to LOX expression in cells, LOX activity was increased in the medium of HLMVECs exposed to HO (3.8 ± 0.2 fold following HO reduced to 2.1 ± 0.2 fold by PF543), which was inhibited by PF543 (figure 4G). As S1P generated in cells is transported to extracellular milieu by S1P transporters,⁴⁷ we investigated the role of the S1P transporter, SPNS2 on LOX expression. Downregulation of SPNS2 by *SPNS2* siRNA reduced HO-mediated LOX expression (2.3 ± 0.3 fold following HO reduced to 1.1 ± 0.2 fold by *siSPNS2*) in HLMVECs (figure 4H,I). Having established a role for SPNS2 in S1P transport and LOX expression, we interrogated the role of extracellular S1P signalling in LOX expression. Exogenous S1P stimulated LOX expression in HLMVECs and HO-induced LOX expression (2.6 ± 0.2 fold) was attenuated by S1P antibody added to the extracellular medium of HLMVECs (1.1 ± 0.1 fold) (figure 4J,K). As extracellular S1P-mediated cellular functions are transduced via G-protein coupled S1P 1–5 receptors, we next investigated the type of S1P receptors involved in HO-induced LOX expression.⁴⁸ Downregulation of S1P₁ with siRNA attenuated HO-induced LOX expression in HLMVECs (3.2 ± 0.2 fold increase following HO reduced to 0.7 ± 0.1 fold by *siS1P₁* under HO) (figure 4L,M). However, knockdown of S1P₂

and S1P₃ with siRNA had no effect on HO-induced LOX expression (data not shown). Collectively, these results suggest involvement of SPHK1/SPNS2/S1P/S1P₁ signalling axis in HO-induced LOX expression in human lung endothelial cells.

SPHK1/S1P signalling regulates HO-induced LOX expression via STAT3 in lung endothelial cells

Activation of S1P₁ by S1P stimulates STAT3 phosphorylation and enhances p-STAT3 colocalisation with S1P₁ in tumour cells.⁴⁹ To determine the potential involvement of STATs in LOX expression, we probed the LOX promoter region by in silico analyses using Genomatix software program, MatInspector. The analyses revealed three different transcript variants of LOX. A matching score was assigned to the transcription factor and the transcript promoter binding/matching probability. A score of 1.00 indicated a perfect match, while the minimum score of 0.8 was considered to be a good match. The results of probing for all the members of the STAT family as potential transcription factors for LOX promoter sites are shown in online supplemental table 3. Sequence GXP_123790 showed a strong correlation for STAT with a matrix similarity score of 0.966 for STAT1. STAT3 showed a near-perfect matching score of 0.968 for transcript 1 and 0.95 for transcript 3 of LOX. Transcript 1 also showed a matching score of 0.966 for STAT1 and transcript 2 showed a matching score of 0.871 for STAT5A (figure 5A,B). Based on the in silico analysis, next we investigated the role of STATs in LOX expression. HLMVECs stimulated by HO (1–6 hours) showed a time-dependent increase in STAT3 phosphorylation peaking at 6 hours (3.4±0.3 fold) (figure 5C,D). Phosphorylation of other STATs was not significantly different between NO and HO exposed HLMVECs (data not shown). Pretreatment of HLMVECs with SPHK1 inhibitor PF543 attenuated HO-induced STAT3 phosphorylation at Tyr 705 (5.9±0.4 fold following HO reduced to 3.1±0.2 fold) (figure 5E,F) and nuclear localisation of p-STAT3 (figure 5G,H) compared with cells exposed to HO but not treated with PF543 (3.3±0.6 fold following HO reduced to 1.8±0.2 fold following PF543). Furthermore, downregulation of STAT3 with siRNA reduced HO-induced LOX expression in HLMVECs (3.1±0.2 fold reduced to 1.2±0.2 fold) (figure 5I,J).

Increased binding of p-STAT3 to the promoter region of LOX

Chromatin immunoprecipitation (ChIP) assay was used to confirm the binding of pSTAT3 to the promoter region of LOX in HLMVEC genome. HO caused increased binding of pSTAT3 to the promoter region of LOX compared with cells exposed to NO (1.7±0.1 fold) (figure 5K). The data were normalised using ‘signal over background’ or ‘relative to the no-antibody control’. Collectively, the above results show a role for SPHK1 signalling in HO-induced STAT3 phosphorylation and binding of STAT3 to LOX promoter in HLMVECs.

DISCUSSION

The pathobiological mechanisms contributing to the remodelling of the ECM and impaired alveolarisation noted in BPD and other lung disorders are poorly understood.^{50 51} In our earlier study, we noted that S1P was elevated in patients with severe BPD and inhibition of SPHK1 by PF543 protected mice against HO-induced BPD as well as airway remodelling.¹⁸ This was accompanied by an amelioration of HO-induced increase in lung

tissue resistance, suggesting a reduction in HO-induced parenchymal damage by PF543 therapy. Formation and remodelling of the ECM are critical processes involving optimal collagen scaffolding, leading to secondary septation of the developing lung necessary for the formation and maturation of alveoli.⁵² The role of copper containing enzyme, LOX, in the remodelling of matrix has been studied in the context of BPD, but the factors regulating LOX that could also incite lung injury in the NB remain unclear.¹⁹ A therapeutic reduction of excessive HO-induced LOX expression and/or activity normalising collagen cross-linking could contribute to improved lung development, as shown in this study. Importantly, we have demonstrated a potential link between SPHK1 and LOX in human BPD. Our collective data support an overall theoretical model for LOX regulation in HO-induced experimental BPD through a novel pathway composed of SPHK1/S1P/S1P₁/STAT3 (figure 6).

Our data clearly demonstrate an upregulation of LOX in neonatal mice with HO-induced lung injury, accompanied by excess collagen deposition and poor alveolar development (figure 2A,B). LOX is essential for normal lung development. Previous studies have clearly identified a key role for LOX and LOXL1 in normal mouse lung development.⁵³ Both these enzymes are temporally regulated and crucial for normal lung embryogenesis, as both *Lox*^{-/-}^{54 55} and *Loxl1*^{-/-}⁵⁶ mouse pups show impaired lung development. Though *Lox*^{-/-} embryos develop to term, they die within hours of birth due to cardiopulmonary failure. LOX plays a key biological role in improving structural integrity of ECM by strengthening the connective tissue. On the contrary, increased LOX is associated with over stabilisation of matrix accompanied by impaired alveolarisation.¹⁹ We noted an elevated expression of *Lox* gene in microarray, and this was confirmed in RT-PCR, as reported by us earlier.⁵⁷ Previous studies revealed increased mRNA expression of *Lox* following both mechanical ventilation and/or HO (40%) in mice.⁵⁰ Interestingly, LOX and LOX-like proteins have also been implicated in intranuclear oxidative deamination of histones. It is beyond the scope of this study to delve into the role of LOX in the nucleus and the epigenetic regulation.

It is interesting to note that the transcriptional regulation of LOX has been reported to be mediated by transforming growth factor (TGF)- β family of growth factors.⁵⁸ TGF- β group of peptide growth factors are also key regulators of late lung development.⁵⁹ Increased TGF- β activity is recognised as a pathogenic factor in animal models of BPD, and downregulation of TGF- β signalling in the NB lung was reported to reduce the expression of the *Lox* gene in the lungs.⁵⁹ Our findings indicate that the regulation of LOX under HO might be overridden by the SPHK1/S1P pathway.

Although there is evidence for the regulation of LOX by TGF- β and NF- κ B in tumours,^{60 61} the data from our study suggest a link between S1P/S1P₁/STAT3 signalling axis and LOX with no role for NF- κ B (figures 4 and 5). Interestingly, S1P/S1P₁ is known to be essential for production of NF- κ B regulated cytokine interleukin-6 secretion via STAT3.⁶⁰ The SPHK1/S1P/S1P₁ axis has been identified as the nexus between NF- κ B and STAT3 signalling in chronic inflammation; however, in this study, we did not note any increase in NF- κ B in response to HO. In addition, inhibition of NF- κ B activation had no impact on LOX expression or activity under HO (data not shown). Thus, under HO regulation of LOX secretion by S1P/S1P₁/STAT3 signalling axis does not involve NF- κ B in HLMVECs. Additionally, here we demonstrate for the first time the link between SPHK1 and LOX

through transcriptional regulation by STAT3 activation under HO using in vitro experiments. In tumour cells, S1P/ S1P₁ induced persistent STAT3 activation.⁶² Inhibition of SPHK1 downregulated HO-induced activation of STAT3, which in turn reduced LOX expression and activity (figures 4 and 5). We have earlier shown elevated expression of SPHK1 and S1P₁ following exposure of neonatal mice to HO.¹³

In addition to the mouse lung, we observed an elevated expression of SPHK1 and LOX in human lung tissues with BPD. This increase in LOX expression in BPD lung specimen is in accordance with previous reports.¹⁹ Here, we link this association by establishing a novel pathway whereby SPHK1/S1P axis regulates the expression of LOX through the S1P₁ and STAT3 pathway. This observation suggests that elevated LOX expression noted in infants with BPD may be attributable to elevated SPHK1 in these neonates. Inhibition of SPHK1 by PF543 protects against BPD-like morphology in neonatal mice associated with reduced LOX, thus suggesting a causal relationship among SPHK1/S1P axis, LOX and BPD. Beyond BPD, PF543 has been shown to reduce pulmonary fibrosis by reducing lung epithelial cell mitochondrial DNA damage and recruitment of fibrogenic monocytes.⁶³

LOX inhibitor β -aminopropionitrile (BAPN), a neurotoxin present in the seeds of *Lathyrus sativus*, is known to cause lathyrism when consumed in large quantities.⁶⁴ Contrary to the expectations, LOX inhibition by BAPN did not protect against hyperoxia-induced BPD,²⁴ though it partially restored normal collagen levels and elastin structure in the developing septa. From this finding it is evident that the mechanism of protection against hyperoxia-induced animal BPD following inhibition of SPHK1 by PF543 is unlikely to be due to LOX inhibition alone. It is pertinent to note that LOX, which is secreted out into the matrix, is by itself capable of generating more ROS, and this could further aggravate or perpetuate the HO-induced injury. LOX also affects the transcriptome relevant to lung development and BPD.⁶⁵ In this context, the protective role of PF543 could be partially attributed to inhibition of LOX secretion.

PF543 has been shown to have its therapeutic effect in various pathological conditions, including inhibition of sickling of erythrocytes in *ex vivo* studies of patients with sickle cell disease.⁴⁵ We have earlier shown that PF543 inhibits SPHK1 and reduces HO-induced ROS formation mediated through p47^{phox} a component of NADPH oxidase.¹³ It is, therefore, very likely that inhibition of SPHK1 that confers protection against HO-induced lung injury may include mechanisms beyond regulation of LOX secretion into the extracellular matrix. Taking into consideration the known mechanisms related to LOX and BPD, it could be deduced that reducing the increased secretion of LOX ameliorates the lung pathology by at least two mechanisms: one by reduced extracellular collagen cross-linking and the other by reduced LOX-induced ROS production. We had earlier shown that genetic deletion of *Sphk2* in neonatal mice was not protective against HO-induced lung injury.¹⁴ In this study, we have shown that inhibition of SPHK1 in *Sphk2*^{-/-} mice protects against HO-induced BPD, thus reiterating the specific role played by SPHK1 in the pathogenesis of BPD. Our delineation of LOX pathway regulation through SPHK1/S1P independent of previously described ones, represents a significant discovery with therapeutic implications.

Limitations

There are several limitations to this study. (1) We excluded patients with pneumonia, pulmonary hypoplasia, congestive cardiac failure and pulmonary hypertension. This limited the patient population available to us. This was done to have a group of patients with BPD alone when it comes to collection of TA or selection of lung specimen for IHC studies. The majority of population that is served by our hospital comprises of patients of African-American or Hispanic background. (2) We have assessed LOX expression or activity in patients with severe BPD only and hence have attempted correlation. However, for IHC, specimens received from the URM repository were included thus diversifying the patient population. (3) Parents of patients who refused to give consent to collect TAs were excluded. Out of a total of five patients with severe BPD from whom we intended to collect TAs during the period of TA collection, two refused. Both parents were of African-American background, and this did not affect the racial/ethnic mix as the three patients from whom the samples were collected are also of same background. (4) Also excluded were patients with pneumonia, pulmonary hypoplasia, congestive cardiac failure and pulmonary hypertension. This limited the patient population available to us. This was done to have a group of patients with BPD alone when it comes to collection of TA or selection of lung specimen for IHC studies. (5) Study of developmental regulation of LOX based on gestational age and developmental expression of SPHK1 is beyond the scope of this manuscript, and study of the same is likely to shed more light into the relationship between SPHK1 and LOX. (6) We have not looked at the therapeutic role of LOX inhibitor compound in enabling lung development in the murine neonatal hyperoxia model, which will be followed in near future.

CONCLUSION

The novel pathway described in this manuscript opens up therapeutic targets at the pretranscriptional and transcriptional regulation level of LOX. We have demonstrated that each step in the SPHK1 pathway that is involved in the S1P synthesis and subsequent transport from inside to the exterior of the cell, followed by subsequent signalling through S1P₁ and STAT3 impacted the expression of LOX. This discovery reveals that one of the critical mechanisms of LOX regulation could involve the SPHK1/S1P signalling pathway in BPD.

Supplementary Material

Refer to Web version on PubMed Central for supplementary material.

Acknowledgements

We gratefully acknowledge the assistance of RRC histology core of University of Illinois, Chicago, and that of University of Chicago in the processing of lung tissue, including immunohistochemistry and image processing. We also gratefully acknowledge the help of Professor Prasad Kanteti, PhD, in editing the manuscript and that of Ms Uma Harijith, MA, in the preparation of this manuscript.

Funding

This work was supported in part by R01HD090887-01A1 from NICHD to AH. The BRINDL repository is funded by NHLBI U01HL122700 and U01HL148861. No role was played by the funding body in the design of the study, collection, analysis and interpretation of data or in writing the manuscript.

Data availability statement

All data relevant to the study are included in the article or uploaded as supplementary information. All data are available and presented with the manuscript.

REFERENCES

1. Andresen JH, Saugstad OD. Oxygen metabolism and oxygenation of the newborn. *Semin Fetal Neonatal Med* 2020;25:101078. [PubMed: 32037265]
2. Bhandari V Hyperoxia-derived lung damage in preterm infants. *Semin Fetal Neonatal Med* 2010;15:223–9. [PubMed: 20430708]
3. Kallet RH, Matthay MA. Hyperoxic acute lung injury. *Respir Care* 2013;58:123–41. [PubMed: 23271823]
4. Ware LB, Matthay MA. The acute respiratory distress syndrome. *N Engl J Med* 2000;342:1334–49. [PubMed: 10793167]
5. Xu X, Han M, Li T, et al. Effective treatment of severe COVID-19 patients with tocilizumab. *Proc Natl Acad Sci U S A* 2020;117:10970–5. [PubMed: 32350134]
6. Mantell LL, Lee PJ. Signal transduction pathways in hyperoxia-induced lung cell death. *Mol Genet Metab* 2000;71:359–70. [PubMed: 11001828]
7. Steinhorn RH, Lakshminrusimha S. Oxygen and pulmonary vasodilation: the role of oxidative and nitrosative stress. *Semin Fetal Neonatal Med* 2020;25:101083. [PubMed: 31983672]
8. Berkelhamer SK, Kim GA, Radder JE, et al. Developmental differences in hyperoxia-induced oxidative stress and cellular responses in the murine lung. *Free Radic Biol Med* 2013;61:51–60. [PubMed: 23499839]
9. Datta A, Kim GA, Taylor JM, et al. Mouse lung development and Nox1 induction during hyperoxia are developmentally regulated and mitochondrial ROS dependent. *Am J Physiol Lung Cell Mol Physiol* 2015;309:L369–77. [PubMed: 26092998]
10. Supplemental therapeutic oxygen for prethreshold retinopathy of prematurity (STOP-ROP), a randomized, controlled trial. I: primary outcomes. *Pediatrics* 2000;105:295–310. [PubMed: 10654946]
11. Hay WW, Bell EF. Oxygen therapy, oxygen toxicity, and the STOP-ROP trial. *Pediatrics* 2000;105:424–5. [PubMed: 10654967]
12. Hilgendorff A, O'Reilly MA. Bronchopulmonary dysplasia early changes leading to long-term consequences. *Front Med* 2015;2:2.
13. Harijith A, Pendyala S, Ebenezer DL, et al. Hyperoxia-induced p47phox activation and ROS generation is mediated through S1P transporter Spns2, and S1P/S1P1&2 signaling axis in lung endothelium. *Am J Physiol Lung Cell Mol Physiol* 2016;311:L337–51. [PubMed: 27343196]
14. Harijith A, Pendyala S, Reddy NM, et al. Sphingosine kinase 1 deficiency confers protection against hyperoxia-induced bronchopulmonary dysplasia in a murine model: role of S1P signaling and Nox proteins. *Am J Pathol* 2013;183:1169–82. [PubMed: 23933064]
15. Ebenezer DL, Berdyshev EV, Bronova IA, et al. *Pseudomonas aeruginosa* stimulates nuclear sphingosine-1-phosphate generation and epigenetic regulation of lung inflammatory injury. *Thorax* 2019;74:579–91. [PubMed: 30723184]
16. Greenough A, Pahuja A. Updates on Functional Characterization of Bronchopulmonary Dysplasia - The Contribution of Lung Function Testing. *Front Med* 2015;2:35.
17. Schmalisch G, Wilitzki S, Roehr CC, et al. Development of lung function in very low birth weight infants with or without bronchopulmonary dysplasia: longitudinal assessment during the first 15 months of corrected age. *BMC Pediatr* 2012;12:37. [PubMed: 22443188]
18. Ha AW, Sudhadevi T, Ebenezer DL, et al. Neonatal therapy with PF543, a sphingosine kinase 1 inhibitor, ameliorates hyperoxia-induced airway remodeling in a murine model of bronchopulmonary dysplasia. *Am J Physiol Lung Cell Mol Physiol* 2020;319:L497–512. [PubMed: 32697651]

19. Kumarasamy A, Schmitt I, Nave AH, et al. Lysyl oxidase activity is dysregulated during impaired alveolarization of mouse and human lungs. *Am J Respir Crit Care Med* 2009;180:1239–52. [PubMed: 19797161]
20. Chen L, Li S, Li W. LOX/LOXL in pulmonary fibrosis: potential therapeutic targets. *J Drug Target* 2019;27:790–6. [PubMed: 30457362]
21. Philp CJ, Siebecke I, Clements D, et al. Extracellular matrix cross-linking enhances fibroblast growth and protects against matrix proteolysis in lung fibrosis. *Am J Respir Cell Mol Biol* 2018;58:594–603. [PubMed: 29053339]
22. López-Jiménez AJ, Basak T, Vanacore RM. Proteolytic processing of lysyl oxidase-like-2 in the extracellular matrix is required for crosslinking of basement membrane collagen IV. *J Biol Chem* 2017;292:16970–82. [PubMed: 28864775]
23. Vallet SD, Miele AE, Uciechowska-Kaczmarzyk U, et al. Insights into the structure and dynamics of lysyl oxidase propeptide, a flexible protein with numerous partners. *Sci Rep* 2018;8:11768. [PubMed: 30082873]
24. Mižíková I, Ruiz-Camp J, Steenbock H, et al. Collagen and elastin cross-linking is altered during aberrant late lung development associated with hyperoxia. *Am J Physiol Lung Cell Mol Physiol* 2015;308:L1145–58. [PubMed: 25840994]
25. Aumiller V, Strobel B, Romeike M, et al. Comparative analysis of lysyl oxidase (like) family members in pulmonary fibrosis. *Sci Rep* 2017;7:149. [PubMed: 28273952]
26. Kasagi Y, Dods K, Wang JX, et al. Fibrostenotic eosinophilic esophagitis might reflect epithelial lysyl oxidase induction by fibroblast-derived TNF- α . *J Allergy Clin Immunol* 2019;144:171–82. [PubMed: 30578874]
27. Hendricks-Muñoz KD, Xu J, Voynow JA. Tracheal aspirate VEGF and sphingolipid metabolites in the preterm infant with later development of bronchopulmonary dysplasia. *Pediatr Pulmonol* 2018;53:1046–52. [PubMed: 29687638]
28. Dautel SE, Kyle JE, Clair G, et al. Lipidomics reveals dramatic lipid compositional changes in the maturing postnatal lung. *Sci Rep* 2017;7:40555. [PubMed: 28145528]
29. Tibboel J, Reiss I, de Jongste JC, et al. Sphingolipids in lung growth and repair. *Chest* 2014;145:120–8. [PubMed: 24394822]
30. Jensen EA, Dysart K, Gantz MG, et al. The diagnosis of bronchopulmonary dysplasia in very preterm infants. an evidence-based approach. *Am J Respir Crit Care Med* 2019;200:751–9. [PubMed: 30995069]
31. Jobe AH, Bancalari E. Bronchopulmonary dysplasia. *Am J Respir Crit Care Med* 2001;163:1723–9. [PubMed: 11401896]
32. Grimm PC, Nickerson P, Gough J, et al. Computerized image analysis of Sirius Red-stained renal allograft biopsies as a surrogate marker to predict long-term allograft function. *J Am Soc Nephrol* 2003;14:1662–8. [PubMed: 12761269]
33. Ambalavanan N, Morty RE. Searching for better animal models of BPD: a perspective. *Am J Physiol Lung Cell Mol Physiol* 2016;311:L924–7. [PubMed: 27663992]
34. Nardiello C, Mižíková I, Silva DM, et al. Standardisation of oxygen exposure in the development of mouse models for bronchopulmonary dysplasia. *Dis Model Mech* 2017;10:185–96. [PubMed: 28067624]
35. Schnute ME, McReynolds MD, Kasten T, et al. Modulation of cellular S1P levels with a novel, potent and specific inhibitor of sphingosine kinase-1. *Biochem J* 2012;444:79–88. [PubMed: 22397330]
36. Usatyuk PV, Burns M, Mohan V, et al. Coronin 1B regulates S1P-induced human lung endothelial cell chemotaxis: role of PLD2, protein kinase C and Rac1 signal transduction. *PLoS One* 2013;8:e63007. [PubMed: 23667561]
37. Huang Y, de Boer WB, Adams LA, et al. Image analysis of liver collagen using Sirius red is more accurate and correlates better with serum fibrosis markers than trichrome. *Liver Int* 2013;33:1249–56. [PubMed: 23617278]
38. Sekhon HS, Keller JA, Proskocil BJ, et al. Maternal nicotine exposure upregulates collagen gene expression in fetal monkey lung. association with alpha7 nicotinic acetylcholine receptors. *Am J Respir Cell Mol Biol* 2002;26:31–41. [PubMed: 11751201]

39. Rosell-Garcia T, Rodriguez-Pascual F. Enhancement of collagen deposition and cross-linking by coupling lysyl oxidase with bone morphogenetic protein-1 and its application in tissue engineering. *Sci Rep* 2018;8:10780. [PubMed: 30018337]
40. Cartharius K, Frech K, Grote K, et al. MatInspector and beyond: promoter analysis based on transcription factor binding sites. *Bioinformatics* 2005;21:2933–42. [PubMed: 15860560]
41. Daiwile AP, Sivanesan S, Tarale P, et al. Role of fluoride induced histone trimethylation in development of skeletal fluorosis. *Environ Toxicol Pharmacol* 2018;57:159–65. [PubMed: 29275289]
42. Wang Y, Ratna P, Shivashankar GV. Superresolution imaging of nanoscale chromosome contacts. *Sci Rep* 2017;7:42422. [PubMed: 28186153]
43. MacRitchie N, Volpert G, Al Washih M, et al. Effect of the sphingosine kinase 1 selective inhibitor, PF-543 on arterial and cardiac remodelling in a hypoxic model of pulmonary arterial hypertension. *Cell Signal* 2016;28:946–55. [PubMed: 27063355]
44. Huang LS, Sudhadevi T, Fu P, et al. Sphingosine kinase 1/S1P signaling contributes to pulmonary fibrosis by activating Hippo/YAP pathway and mitochondrial reactive oxygen species in lung fibroblasts. *Int J Mol Sci* 2020;21. doi:10.3390/ijms21062064. [Epub ahead of print: 17 Mar 2020].
45. Zhang Y, Berka V, Song A, et al. Elevated sphingosine-1-phosphate promotes sickling and sickle cell disease progression. *J Clin Invest* 2014;124:2750–61. [PubMed: 24837436]
46. Pyne NJ, McNaughton M, Boomkamp S, et al. Role of sphingosine 1-phosphate receptors, sphingosine kinases and sphingosine in cancer and inflammation. *Adv Biol Regul* 2016;60:151–9. [PubMed: 26429117]
47. Fu P, Ebenezer DL, Berdyshev EV, et al. Role of sphingosine kinase 1 and S1P transporter SPNS2 in HGF-mediated lamellipodia formation in lung endothelium. *J Biol Chem* 2016;291:27187–203. [PubMed: 27864331]
48. Rosen H, Goetzl EJ. Sphingosine 1-phosphate and its receptors: an autocrine and paracrine network. *Nat Rev Immunol* 2005;5:560–70. [PubMed: 15999095]
49. Tsai H-C, Nguyen K, Hashemi E, et al. Myeloid sphingosine-1-phosphate receptor 1 is important for CNS autoimmunity and neuroinflammation. *J Autoimmun* 2019;105:102290. [PubMed: 31202617]
50. Bland RD, Ertsey R, Mokres LM, et al. Mechanical ventilation uncouples synthesis and assembly of elastin and increases apoptosis in lungs of newborn mice. prelude to defective alveolar septation during lung development? *Am J Physiol Lung Cell Mol Physiol* 2008;294:L3–14. [PubMed: 17934062]
51. Witsch TJ, Turowski P, Sakkas E, et al. Deregulation of the lysyl hydroxylase matrix cross-linking system in experimental and clinical bronchopulmonary dysplasia. *Am J Physiol Lung Cell Mol Physiol* 2014;306:L246–59. [PubMed: 24285264]
52. Thibeault DW, Mabry SM, Ekekezie II, et al. Collagen scaffolding during development and its deformation with chronic lung disease. *Pediatrics* 2003;111:766–76. [PubMed: 12671110]
53. Kho AT, Bhattacharya S, Mecham BH, et al. Expression profiles of the mouse lung identify a molecular signature of time-to-birth. *Am J Respir Cell Mol Biol* 2009;40:47–57. [PubMed: 18664640]
54. Hornstra IK, Birge S, Starcher B, et al. Lysyl oxidase is required for vascular and diaphragmatic development in mice. *J Biol Chem* 2003;278:14387–93. [PubMed: 12473682]
55. Mäki JM, Räsänen J, Tikkanen H, et al. Inactivation of the lysyl oxidase gene LOX leads to aortic aneurysms, cardiovascular dysfunction, and perinatal death in mice. *Circulation* 2002;106:2503–9. [PubMed: 12417550]
56. Liu X, Zhao Y, Gao J, et al. Elastic fiber homeostasis requires lysyl oxidase-like 1 protein. *Nat Genet* 2004;36:178–82. [PubMed: 14745449]
57. Ebenezer DL, Fu P, Krishnan Y, et al. Genetic deletion of SphK2 confers protection against *Pseudomonas aeruginosa* mediated differential expression of genes related to virulent infection and inflammation in mouse lung. *BMC Genomics* 2019;20:984. [PubMed: 31842752]

58. Xu X-H, Jia Y, Zhou X, et al. Downregulation of lysyl oxidase and lysyl oxidase-like protein 2 suppressed the migration and invasion of trophoblasts by activating the TGF- β /collagen pathway in preeclampsia. *Exp Mol Med* 2019;51:1–12.
59. Saito A, Horie M, Nagase T. TGF- β Signaling in Lung Health and Disease. *Int J Mol Sci* 2018;19. doi:10.3390/ijms19082460. [Epub ahead of print: 20 Aug 2018].
60. Liang J, Nagahashi M, Kim EY, et al. Sphingosine-1-Phosphate links persistent STAT3 activation, chronic intestinal inflammation, and development of colitis-associated cancer. *Cancer Cell* 2013;23:107–20. [PubMed: 23273921]
61. Jeong YJ, Park SH, Mun SH, et al. Association between lysyl oxidase and fibrotic focus in relation with inflammation in breast cancer. *Oncol Lett* 2018;15:2431–40. [PubMed: 29434955]
62. Lee H, Deng J, Kujawski M, et al. STAT3-induced S1PR1 expression is crucial for persistent STAT3 activation in tumors. *Nat Med* 2010;16:1421–8. [PubMed: 21102457]
63. Cheresh P, Kim S-J, Huang LS, et al. The sphingosine kinase 1 inhibitor, PF543, mitigates pulmonary fibrosis by reducing lung epithelial cell mtDNA damage and recruitment of fibrogenic monocytes. *Int J Mol Sci* 2020;21. doi:10.3390/ijms21165595. [Epub ahead of print: 05 Aug 2020].
64. Herchenhan A, Uhlenbrock F, Eliasson P, et al. Lysyl oxidase activity is required for ordered collagen fibrillogenesis by tendon cells. *J Biol Chem* 2015;290:16440–50. [PubMed: 25979340]
65. Mižiková I, Palumbo F, Tábi T, et al. Perturbations to lysyl oxidase expression broadly influence the transcriptome of lung fibroblasts. *Physiol Genomics* 2017;49:416–29. [PubMed: 28698228]

Key messages

What is the key question?

- How does sphingosine kinase 1 (SPHK1) contribute to the pathobiology of neonatal bronchopulmonary dysplasia (BPD) by regulating lysyl oxidase (LOX)?

What is the bottom line?

- SPHK1 is increased in lung tissue of human BPD. An associated increase of LOX in human tissue correlated well with similar findings in mouse lung. We found that SPHK1/sphingosine-1-phosphate (S1P)/S1P receptor 1 signalling axis regulates LOX through STAT3.

Why read on?

- The manuscript reveals a novel pathway depicting the transcriptional regulation of LOX by SPHK1 through STAT3.

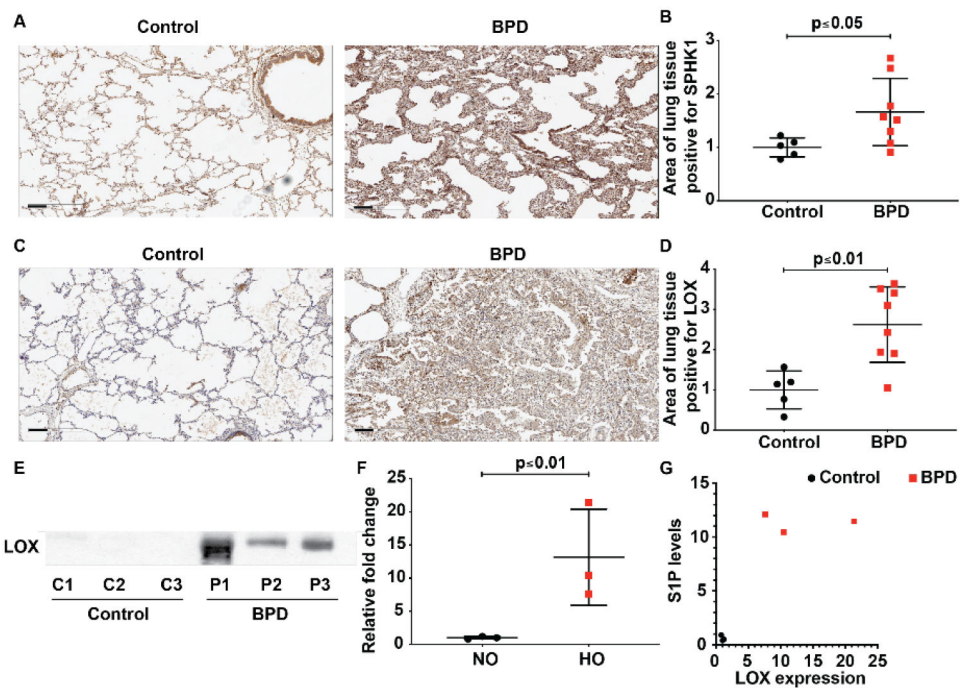


Figure 1.

Elevated sphingosine kinase 1 (SPHK1) and lysyl oxidase (LOX) expression are noted in lung tissue of neonates with severe BPD. Paraffin-embedded lung sections were used to assess expression of SPHK1 (A) and LOX by immunohistochemistry (C) in the lung tissue of neonates with BPD compared with controls. Intensity of antibody staining (brown) was quantified in halo system using scanned lung images (B and D). LOX was also elevated in the tracheal aspirates of newborns with severe BPD (E). Quantified data show significance (F). Correlation test showed significant relationship ($r=0.831$) between LOX content in TA detected by immunoblot and the S1P level estimated (G). Original view, 10 \times , scale bar 100 μ m. Statistical analyses done with Pearson correlation and Mann-Whitney U test. Details of patients are given in online supplemental tables 12. BPD, bronchopulmonary dysplasia; S1P, sphingosine-1-phosphate.

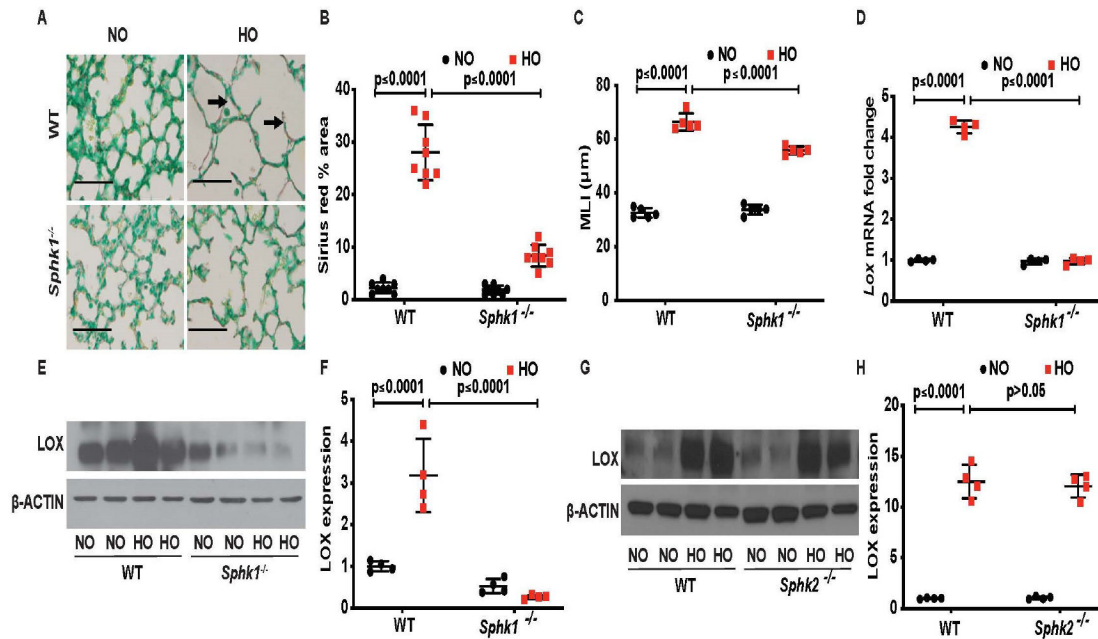


Figure 2.

Deletion of sphingosine kinase 1 gene (*Sphk1*^{-/-}) protects alveolarisation of murine neonatal lungs under hyperoxia (HO) accompanied by reduced collagen deposition/cross-linking. Representative H&E photomicrographs of lung sections from neonatal wild type (WT) and *Sphk1*^{-/-} mice, exposed to room air or hyperoxia (HO) stained with sirius red for collagen (dark arrow). *Sphk1*^{-/-} KO exposed to HO showed improved alveolarisation accompanied by reduced sirius red staining (A). The objective assessment of sirius red staining of the lungs was determined by quantification using ImageJ system. Following exposure to HO, sirius red staining of the lung of *Sphk1*^{-/-} newborn mice is significantly lower compared with WT control exposed to HO (B) accompanied by protection against HO-induced lung injury as evidenced by improved mean linear intercept suggestive of improved alveolarisation (C). RT-PCR showed an increase in expression of *Lox* following HO in the WT, which was not seen in the *Sphk1*^{-/-} exposed to HO (D). Whole lung tissue lysates subjected to SDS-PAGE and western blotting showed increased expression of LOX following HO in WT compared with no controls. This increase in expression was significantly reduced in the *Sphk1*^{-/-} KO exposed to HO (E and F). Western blotting showed increased expression of LOX following HO in *Sphk2*^{-/-} compared with no controls quite similar to the expression seen in WT (G and H). Original view, 40×, scale bar 100 μm. Statistical analyses done with two-way analysis of variance test, N 6–8/group, equal number of males and females used.

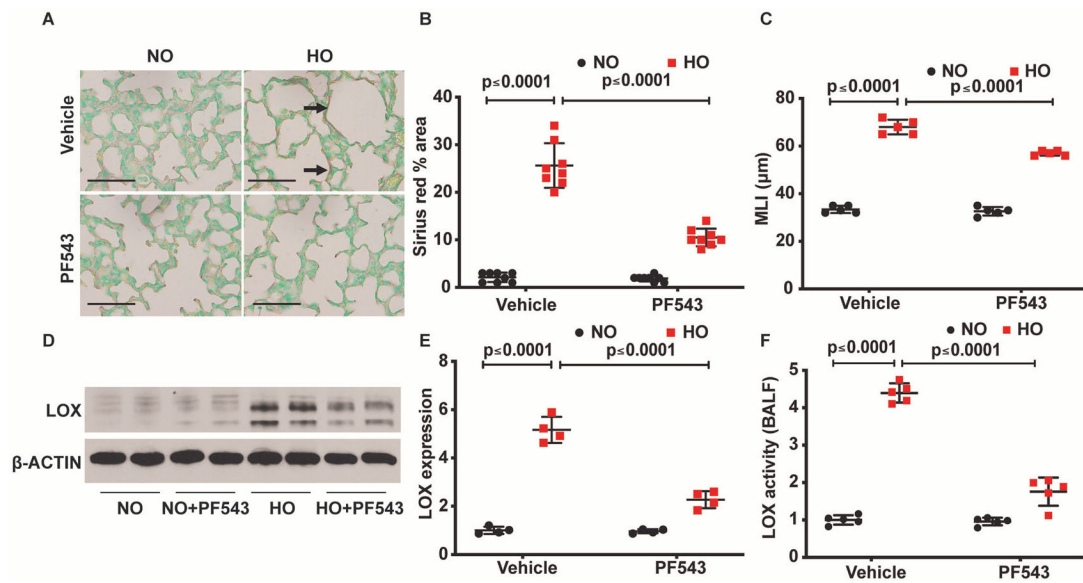


Figure 3.

Inhibition of sphingosine kinase 1 protects alveolarisation of murine neonatal lungs under hyperoxia (HO) accompanied by reduced collagen deposition/cross-linking. Representative H&E photomicrographs of sirius red stained (dark arrow) lung sections from neonatal wild type (WT) mice, exposed to RA or HO and treated with PF543 or vehicle. WT pups exposed to HO but treated with PF543 showed improved alveolarisation accompanied by reduced sirius red staining (A). Quantified data of sirius red staining of the lungs were determined using ImageJ system. Following exposure to HO, sirius red staining of the lung of PF543-treated newborn mice is significantly lower compared with WT control exposed to HO (B). This was accompanied by protection against HO induced lung injury as evidenced by improved MLI suggestive of improved alveolarisation (C). Whole lung tissue lysates subjected to SDS-PAGE and western blotting showed increased expression of lysyl oxidase (LOX) following HO in WT compared with no controls. This increase in expression was significantly reduced in the WT exposed to HO and treated with PF543 (D and E). The reduction of expression of LOX in lung tissue lysates in the western blot of HO exposed and PF543 treated was accompanied by reduced LOX activity in the bronchoalveolar lavage fluid (F). Original view, 40 \times , scale bar 100 μ m. Statistical analyses done with two-way analysis of variance test, N 6–8/group, equal number of males and females used.

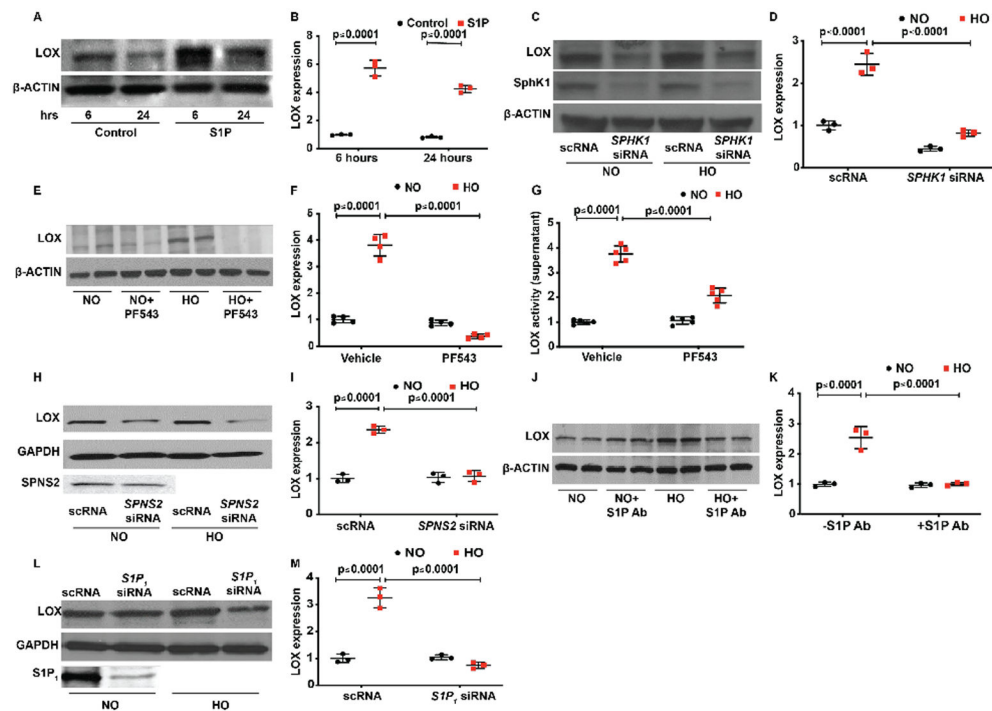


Figure 4.

Interruption of the SPHK1/S1P signalling pathway attenuates HO-induced increased LOX expression in human primary lung microvascular endothelial cells (HLMVECs). HLMVECs were used to study the influence of SPHK1/S1P signalling on LOX production. Exogenous S1P added to HLMVECs resulted in an increased expression of LOX at 6 hours, and there was no further increase noted at 24 hours (A and B). HO-induced increased expression of LOX at 6 hours was reduced by *SPHK1 siRNA* (C and D). Similar to the effect of siRNA, SPHK1 inhibitor, PF543, also prevented a HO-induced increase in LOX expression. No difference was noted between the two groups pretreated with or without PF543 (E and F). In consonance with a reduction of HO-induced expression of LOX following PF543 therapy, there was a significant reduction of LOX activity in the cell culture supernatant as well following PF543 therapy and exposure to HO (G). S1P transporter SPNS2 transporting S1P from inside the cell to the outside enabling it to bind to S1P receptors. *siSPNS2* reduced HO-induced increased expression of LOX (H and I). S1P binding antibodies were added to the medium prior to exposure of HLMVECs to HO. Following exposure to HO, S1P antibody added group showed a reduced expression of LOX suggesting a role for S1P transported out of the cell into the medium in regulating LOX expression (J and K). *siS1P₁* reduced HO-induced increased expression of LOX compared with HO and NO controls (L and M). Statistical analyses done with two-way analysis of variance test. Images for control and treatment groups in microscopy experiments were collected at the same time under the same conditions. HO, hyperoxia; LOX, lysyl oxidase; NO, normoxia; S1P, sphingosine-1-phosphate receptor 1; SPHK1, sphingosine kinase 1.

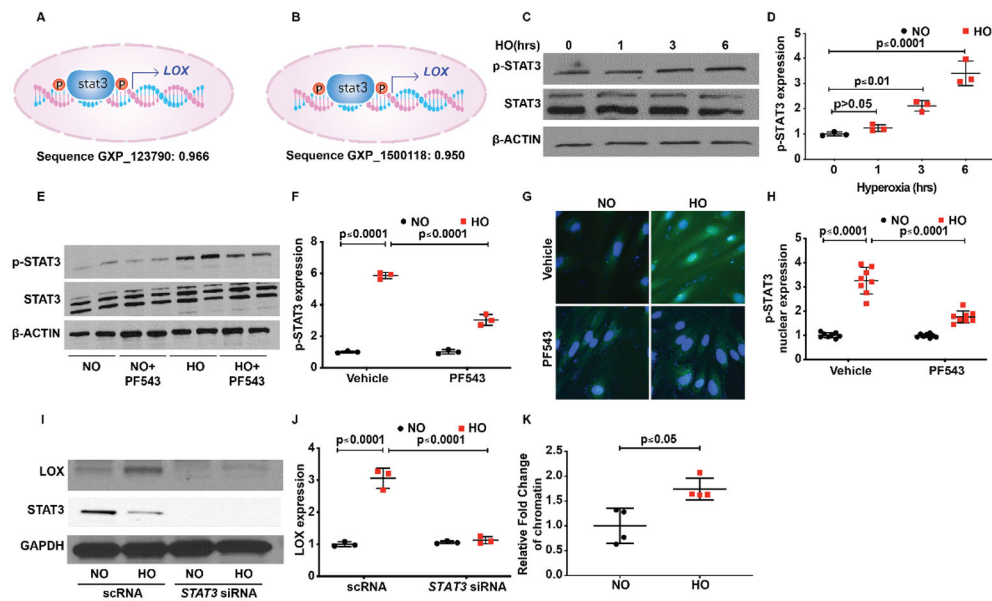


Figure 5.

Transcription factor STAT3 serves to activate S1P-mediated *LOX* transcription leading to HO-induced increased *LOX* expression in human primary lung microvascular endothelial cells (HLMVECs). In silico analyses showed a strong probability for STAT3 binding to the promoter site of *LOX* with a score of 0.966 and 0.95 (A and B). HLMVECs exposed to HO showed activation of STAT3 at 3 hours of HO as evidenced by its translocation to the nucleus, which was inhibited by PF543 the SPHK1 inhibitor (C and D; G & H). HO induced an increase in expression of pSTAT3, which peaked at 6 hours. PF543 inhibited HO-induced increased expression of pSTAT3 at 6 hours (E and F). *siSTAT3* inhibited HO-induced increased expression of *LOX* (I and J). Chromatin immune precipitation assay was done after 3 hours of HO, which showed a 1.7-fold increase in enrichment of STAT3 in the *LOX* promoter region. HO, hyperoxia; *LOX*, lysyl oxidase; NO, normoxia; S1P, sphingosine-1-phosphate receptor 1.

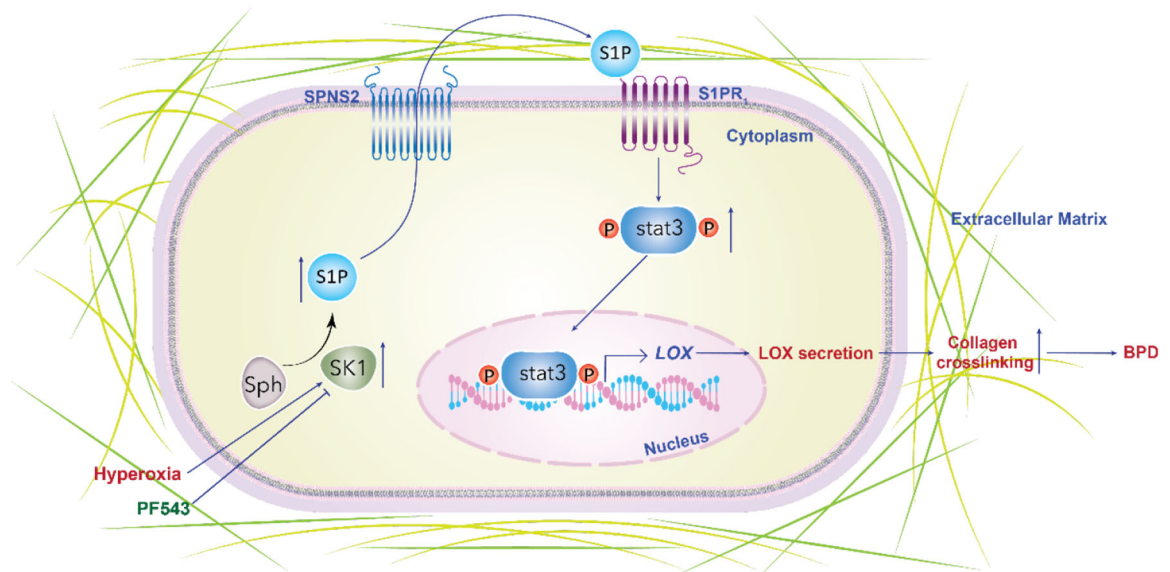


Figure 6.

Schema showing the summary of the theoretical model of SPHK1/S1P/STAT3 axis in regulating LOX HO-induced experimental BPD. HO causes an increase in SPHK1, which stimulates the formation of S1P. HO leads to increased production of LOX leading to increased collagen cross-linking as evidenced by increased sirius red staining driven by SPHK1, S1P, SPNS2, S1P receptor 1 and STAT3 pathway. Inhibition of this pathway along its various components was associated with reduced LOX expression. Inhibition of SPHK1 was associated with reduced LOX production and collagen staining of lung tissue accompanied by restoration of lung alveolarisation. BPD, bronchopulmonary dysplasia; HO, hyperoxia; LOX, lysyl oxidase; S1P, sphingosine 1 phosphate; SPHK1, sphingosine kinase 1.